# A palmitoylation cycle dynamically regulates partitioning of the GABA-synthesizing enzyme GAD65 between ER-Golgi and post-Golgi membranes

**Jamil Kanaani[1,2], George Patterson[3], Fred Schaufele[1], Jennifer Lippincott-Schwartz[3] and Steinunn Baekkeskov[1,2,*]**

[1]Department of Medicine and Diabetes Center, [2]Department of Microbiology and Immunology, University of California San Francisco, 513 Parnassus Avenue, HSW 1090, San Francisco, CA 94143-0534, USA
[3]Cell Biology and Metabolism Branch, National Institute of Child Health and Human Development, National Institutes of Health, Bethesda, MD 21218, USA
*Author for correspondence (e-mail: s_baekkeskov@biochem.ucsf.edu)

## Summary

GAD65, the smaller isoform of the enzyme glutamic acid decarboxylase, synthesizes GABA for fine-tuning of inhibitory neurotransmission. GAD65 is synthesized as a soluble hydrophilic protein but undergoes a hydrophobic post-translational modification and becomes anchored to the cytosolic face of Golgi membranes. A second hydrophobic modification, palmitoylation of Cys30 and Cys45 in GAD65, is not required for the initial membrane anchoring but is crucial for post-Golgi trafficking of the protein to presynaptic clusters. The mechanism by which palmitoylation directs targeting of GAD65 through and out of the Golgi complex is unknown. Here, we show that prior to palmitoylation, GAD65 anchors to both ER and Golgi membranes. Palmitoylation, however, clears GAD65 from the ER-Golgi, targets it to the *trans*-Golgi network and then to a post-Golgi vesicular pathway. FRAP analyses of trafficking of GAD65-GFP reveal a rapid and a slow pool of protein replenishing the Golgi complex. The rapid pool represents non-palmitoylated hydrophobic GAD65-GFP, which exchanges rapidly between the cytosol and ER/Golgi membranes. The slow pool represents palmitoylation-competent GAD65-GFP, which replenishes the Golgi complex via a non-vesicular pathway and at a rate consistent with a depalmitoylation step. We propose that a depalmitoylation-repalmitoylation cycle serves to cycle GAD65 between Golgi and post-Golgi membranes and dynamically control levels of enzyme directed to the synapse.

Supplementary material available online at http://jcs.biologists.org/cgi/content/full/121/4/437/DC1

Key words: Glutamic acid decarboxylase, Palmitoylation signals, Palmitoylation cycle, Membrane trafficking, ER/Golgi trafficking, Golgi/post-Golgi cycling, FRAP analysis.

## Introduction

The inhibitory neurotransmitter γ-amino butyric acid (GABA) is synthesized by two highly homologous isoforms of the pyridoxal 5′ phosphate (PLP)-dependent enzyme glutamic acid decarboxylase, GAD65 and GAD67. GAD67 is constitutively active and synthesizes ~90% of the basal GABA pool in the adult mouse brain. Ablation of *GAD67* (also known as *Gad1*) in the mouse results in neonatal lethality (Condie et al., 1997; Asada et al., 1997). By contrast, *GAD65* (also known as *Gad2*), an autoantigen in human type 1 diabetes (Baekkeskov et al., 1990) and stiff-person syndrome (Solimena et al., 1990), provides GABA for the fine-tuning of inhibitory neurotransmission and appears to be under a tight regulatory control. *GAD65*^{−/−} mice develop normally but are prone to epilepsy, anxiety, and subtle defects in control of behavior and responses to environmental stimuli (Asada et al., 1996; Kash et al., 1997; Kash et al., 1999; Hensch et al., 1998; Stork et al., 2000; Stork et al., 2003; Shimura et al., 2004). Furthermore, GABA synthesized by GAD65 is critical for sustaining intense inhibitory neurotransmission (Tian et al., 1999; Patel et al., 2006). Two qualities of GAD65 may be important in this respect. First, although the majority of GAD67 is constitutively

active, a large fraction of GAD65 in brain is present as an inactive apoenzyme and provides a pool for rapid activation by influx of PLP to form the holoenzyme (Battaglioli et al., 2003). Furthermore, the targeting of the enzyme to membranes of synaptic vesicles that store and secrete its product GABA may provide for a rapid delivery of GABA synthesized by activated GAD65 in response to a sudden increase in demand.

GAD65 is targeted to presynaptic clusters in axons (Kanaani et al., 2002) and synaptic-like microvesicles in pancreatic β cells (Reetz et al., 1991; Christgau et al., 1992) by a mechanism involving several steps. A schematic model for the post-translational modification and trafficking of GAD65 is shown in Fig. 1. GAD65 is synthesized as a hydrophilic soluble protein, Form 1 (F1), which undergoes at least two steps of hydrophobic post-translational modifications in the N-terminal domain (Christgau et al., 1991; Christgau et al., 1992). The first step involves an irreversible and as yet undefined hydrophobic modification in the cytosol (Step A) and results in a hydrophobic form, F2, that anchors to Golgi membranes (Christgau et al., 1991; Christgau et al., 1992; Kanaani et al., 2002). This form, which is not palmitoylated, has weak membrane avidity and can be released
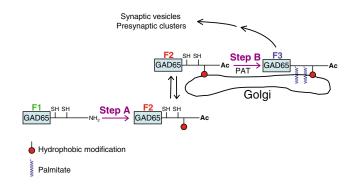
**Fig. 1.** Schematic model of post-translational modification and subcellular targeting of GAD65. Newly synthesized hydrophilic and soluble GAD65 (F1) undergoes an irreversible hydrophobic modification in the cytosol (Step A). The resulting hydrophobic GAD65 (F2) reversibly associates with Golgi membranes. In Golgi membranes, the protein undergoes palmitoylation (Step B) catalyzed by a palmitoyl transferase (PAT). The palmitoylated protein (F3) is targeted out of the Golgi compartment and to a pathway to synaptic vesicles and presynaptic termini in neurons and synaptic-like microvesicles in pancreatic β cells.

from membranes in the absence of detergents (Christgau et al., 1991; Christgau et al., 1992). The second step of post-translational modifications (Step B) results in a firmly membrane-anchored protein, F3, which is only released from membranes by detergent (Christgau et al., 1991; Christgau et al., 1992). A fraction of this membrane-anchored pool of the protein is palmitoylated (Christgau et al., 1992; Shi et al., 1994). However, palmitoylation is not critical for membrane anchoring (Shi et al., 1994; Solimena et al., 1994; Kanaani et al., 2002; Kanaani et al., 2004). Three distinct trafficking signals have been identified in the N-terminal domain of GAD65 (Kanaani et al., 2002). A Golgi-targeting sequence residing in the first 23 amino acids and a membrane-anchoring signal residing in residues 24-31 are required for targeting to Golgi membranes (Shi et al., 1994; Solimena et al., 1994; Kanaani et al., 2002). The third signal, involving palmitoylation of Cys30 and Cys45 (Shi et al., 1994) is critical for trafficking of the protein from Golgi membranes to presynaptic clusters in axon termini (Kanaani et al., 2002) by a Rab5a-dependent pathway (Kanaani et al., 2004). In addition to the hydrophobic post-translational modifications, GAD65 is phosphorylated on Ser3, Ser6, Ser10 and Ser13 (Namchuk et al., 1997) and acetylated on the penultimate alanine following removal of the N-terminal methionine (Battaglioli et al., 2005). The role of these modifications is unknown.

Both wild-type (wt) GAD65 and a palmitoylation-deficient mutant, GAD65(C30,45A), anchor to Golgi membranes, and subcellular fractionation and detergent extraction of membranes have not revealed significant differences in their membrane affinity (Shi et al., 1994; Kanaani et al., 2002) (and our unpublished results). However, only the palmitoylated form of GAD65 traffics beyond the Golgi complex. In this study, we focus on elucidating the steps involved in trafficking of GAD65 into, through and out of the Golgi complex. We show that prior to palmitoylation, GAD65 associates with both endoplasmic reticulum (ER) and Golgi membranes and undergoes a rapid, continuous exchange between the cytosol and Golgi membranes. Palmitoylation, however, shifts the protein to the *trans*-Golgi network (TGN) and a post-Golgi vesicular pathway. Using a FRAP protocol, developed to study cycling of NRAS and HRAS between the plasma membrane and Golgi complex, we show evidence to suggest that

palmitoylated GAD65 cycles back to the Golgi complex with recovery kinetics consistent with a non-vesicular pathway and a depalmitoylation step. The data fit a model, first proposed for cycling of NRAS and HRAS (Goodwin et al., 2005; Rocks et al., 2005) between Golgi and plasma membranes, by which a cycle of depalmitoylation-repalmitoylation regulates the distribution of GAD65 between a vesicular pathway destined for presynapses and the Golgi complex.

## Results

### Palmitoylation-deficient GAD65 associates with both ER and Golgi membranes whereas palmitoylation clears GAD65 from ER membranes

Earlier studies have shown that wt GAD65-GFP is predominantly located in Golgi membranes and in presynaptic clusters in neurons, whereas the palmitoylation-deficient GAD65(C30,45A)-GFP fusion protein is detected in a diffuse pattern in the cytosol as well as in Golgi membranes (Kanaani et al., 2002; Kanaani et al., 2004). This difference suggested that a significant fraction of the protein is soluble in the absence of palmitoylation. However, subcellular fractionation studies failed to detect differences in the ratio of soluble and membrane-bound pools of wt and palmitoylation-deficient GAD65 (Shi et al., 1994) (and our unpublished results). We therefore re-examined the localization of wt and palmitoylation-deficient GAD65-GFP using enhanced resolution confocal analyses of fixed neurons and COS-7 cells. Those analyses confirmed the location of palmitoylation-deficient GAD65 in Golgi membranes but also revealed the cytosolic localization in a fine mesh of membranes reminiscent of the ER. Coexpression of palmitoylation-deficient GAD65(C30,45A)-GFP with the ER marker DsRed2-ER in neurons and COS-7 cells showed extensive colocalization in ER membranes of both cell types (Fig. 2A,C,E). Thus, the hydrophobic but palmitoylation-deficient GAD65(C30,45A)-GFP protein anchors to both ER and Golgi membranes. By contrast, wt GAD65-GFP localized predominantly to Golgi membranes in the cell body of neurons and COS-7 cells and colocalization with DsRed2-ER was rare (Fig. 2B,D,E). Therefore, at steady state, the local concentrations of wt GAD65-GFP in endomembranes is shifted from ER to Golgi membranes much as has been reported for palmitoylation competent GFP-NRAS (Choy et al., 1999). This result suggests that the first hydrophobic modification of GAD65 targets the protein to both ER and Golgi membranes whereas the subsequent palmitoylation of GAD65 serves to clear the protein out of ER membranes.
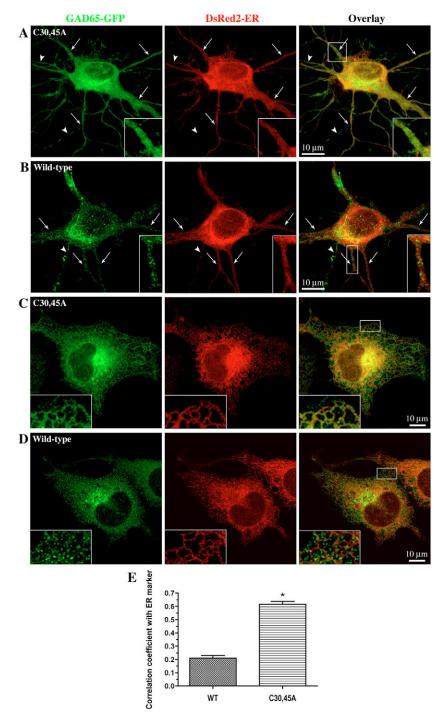
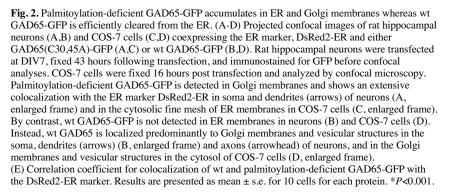### Palmitoylation is required for vesicular trafficking of GAD65-GFP

The enhanced resolution confocal analyses also revealed wt GAD65-GFP in vesicular structures in the cytosol (Fig. 2B,D, see insets). Vesicular structures containing wt GAD65-GFP were detected in axons of all transfected neurons as well as in the soma and dendrites of a subset of neurons (Fig. 3A, see also Fig. 2B, Fig. 4C,D). GAD65-GFP-positive vesicles were also detected in the cytoplasm of fixed MDCK and COS-7 cells (Fig. 3C,E,G). By contrast, palmitoylation-deficient GAD65-GFP was not detected in vesicles in any of the three cell types (Fig. 3B,D,F,G; see also Fig. 2A,C, and Fig. 4A,B) and instead remained in the Golgi and ER compartments.

To confirm this observation, high-resolution confocal microscopy was used in real time to image live-cell hippocampal neurons revealing a bi-directional movement of GAD65-GFP-

containing vesicles in somatodendritic as well as axonal compartments (supplementary material Movie 1). In live COS-7 and MDCK cells, palmitoylated GAD65-GFP-containing vesicles appeared to move randomly in the cytosol (supplementary material Movie 2 and results not shown). By contrast, as observed for fixed cells, the palmitoylation-deficient protein was not detected in vesicles in live neurons, COS-7 or MDCK cells (supplementary material Movie 3, and results not shown).

## Palmitoylation results in a spatially distinct localization of GAD65-GFP in Golgi membranes and colocalization with TGN markers

Cholesterol depletion results in severe impairment of trafficking of wild-type GAD65 from Golgi membranes to presynaptic clusters, suggesting that sorting of palmitoylated GAD65 into cholesterol-rich membrane microdomains is a crucial step in its trafficking pathway (Kanaani et al., 2002). We speculated that palmitoylation mediates sorting of GAD65 into membrane microdomains in the TGN and that this translocation enables the protein to enter a vesicular pathway exiting the Golgi. To address this possibility, we asked whether wt and palmitoylation-deficient GAD65 localize to geometrically distinct parts of Golgi membranes. Both wt *GAD65-GFP* and palmitoylation-deficient *GAD65-GFP* fusion genes were transfected into primary rat hippocampal neurons, COS-7 cells or MDCK cells and the localization of their gene products in Golgi membranes was compared with that of the *cis*-Golgi matrix protein GM130 and the *trans*-Golgi network protein TGN38 using high-resolution confocal microscopy (Fig. 4). Double immunofluorescence analyses revealed a spatial difference in the localization of wt and palmitoylation-deficient GAD65-GFP in Golgi membranes compared with those markers. Palmitoylation-deficient GAD65-GFP formed a ribbon-like staining juxtaposed to the *trans*-Golgi protein TGN38 (Fig. 4A) and the *cis*-Golgi protein GM130 (Fig. 4B). The wt GAD65-GFP, however, colocalized with TGN38 (Fig. 4C,E). Although neither wt nor palmitoylation-deficient GAD65-GFP colocalized with GM130 (Fig. 4B,D, supplementary material Fig. S1), their localization appeared to be on the opposite faces of this marker protein (compare Fig. 4B with 4D). The difference in spatial localization between wt and palmitoylation-deficient GAD65-GFP was also observed in the Golgi compartment of COS-7 and MDCK cells (results not shown). The spatial localization of GAD65(C30,45A)-GFP compared with TGN38 and GM130 was similar to that of the *cis*-Golgi



**Fig. 2.** Palmitoylation-deficient GAD65-GFP accumulates in ER and Golgi membranes whereas wt GAD65-GFP is efficiently cleared from the ER. (A-D) Projected confocal images of rat hippocampal neurons (A,B) and COS-7 cells (C,D) coexpressing the ER marker, DsRed2-ER and either GAD65(C30,45A)-GFP (A,C) or wt GAD65-GFP (B,D). Rat hippocampal neurons were transfected at DIV7, fixed 43 hours following transfection, and immunostained for GFP before confocal analyses. COS-7 cells were fixed 16 hours post transfection and analyzed by confocal microscopy. Palmitoylation-deficient GAD65-GFP is detected in Golgi membranes and shows an extensive colocalization with the ER marker DsRed2-ER in soma and dendrites (arrows) of neurons (A, enlarged frame) and in the cytosolic fine mesh of ER membranes in COS-7 cells (C, enlarged frame). By contrast, wt GAD65-GFP is not detected in ER membranes in neurons (B) and COS-7 cells (D). Instead, wt GAD65 is localized predominantly to Golgi membranes and vesicular structures in the soma, dendrites (arrows) (B, enlarged frame) and axons (arrowhead) of neurons, and in the Golgi membranes and vesicular structures in the cytosol of COS-7 cells (D, enlarged frame).
(E) Correlation coefficient for colocalization of wt and palmitoylation-deficient GAD65-GFP with the DsRed2-ER marker. Results are presented as mean ± s.e. for 10 cells for each protein. *P<0.001.
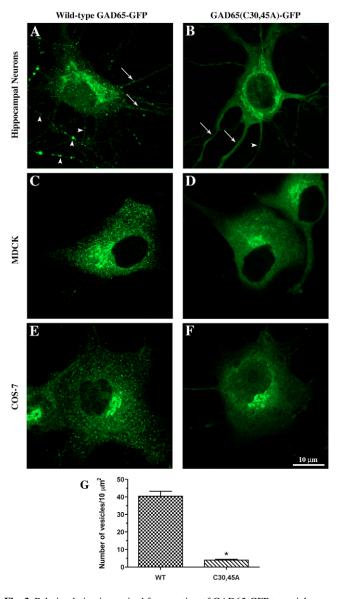
**Wild-type GAD65-GFP**   **GAD65(C30,45A)-GFP**



**Fig. 3.** Palmitoylation is required for targeting of GAD65-GFP to vesicles. (A-F) Projected confocal images of rat hippocampal neurons (A,B), MDCK cells (C,D) and COS-7 cells (E,F), transiently expressing either wt GAD65-GFP (A,C,E) or the palmitoylation-deficient mutant GAD65(C30,45A)-GFP (B,D,F). Rat hippocampal neurons were transfected at DIV6, fixed 72 hours following transfection and immunostained for GFP before confocal analyses. COS-7 and MDCK cells were fixed 18 hours post-transfection and analyzed by confocal microscopy. In addition to Golgi localization, GAD65-GFP-containing vesicles were observed in soma, dendrites (arrows) and axons (arrowheads) of rat hippocampal neurons and in the cytoplasm of fixed COS-7 and MDCK cells (see also supplementary material Movies 1 and 2). By contrast, palmitoylation-deficient GAD65-GFP was detected in Golgi membranes and in a diffuse pattern throughout the cell but not in vesicles in any of the three cell types (see also supplementary material Movie 3). (G) Quantification of wt GAD65-GFP and GAD65(C30,45A)-GFP positive vesicles in the cytosol of COS-7 cells. Results are presented as mean ± s.e. for five cells for each protein. *$P<0.001$.

protein CASP, compared with the same markers (supplementary material Fig. S2). However, the spatial localization of wt GAD65-GFP with GM130 was similar to that of the synaptic vesicle membrane proteins VGAT-HA and VAMP2-GFP as well as the dominant negative mutant of Rab5a, GFP-Rab5a(S34N),

compared with the same markers (supplementary material Fig. S3).

The compound Brefeldin A (BFA) inactivates the small GTPase ADP-ribosylation factor 1 (Arf1), blocks export from the ER and results in a reversible distribution of the Golgi complex into the ER (for a review, see Klausner et al., 1992). However, the TGN does not redistribute into the ER (Chege and Pfeffer, 1990) and instead fuses with early endosomal membranes (Wood et al., 1991; Lippincott-Schwartz et al., 1991). In the presence of BFA, live-cell imaging reveals a major difference in the dissociation rate of membrane proteins residing in the TGN and different parts of the Golgi compartment. A peripheral *cis*-Golgi protein, Arf1, disperses quickly into the cytosol (Vasudevan et al., 1998), whereas the resident Golgi transmembrane enzyme β1,4-galactosyltransferase 1 (GalT) redistributes at a slower rate into the ER (Klausner et al., 1992). By contrast, only a fraction of TGN membrane proteins disperses into the ER and the majority remains in tubular structures representing TGN fused with endosomal membranes. Thus, BFA treatment separates proteins in the TGN from the rest of the Golgi proteins (Chege and Pfeffer, 1990). We used live-cell imaging to determine whether wt and palmitoylation-deficient GAD65-GFP behave differently in the presence of BFA, using Arf1 and GalT, each tagged with a monomeric red fluorescent protein (Arf1-mRFP1 and GalT-mRFP1) as dynamic localization controls (Fig. 5 and supplementary material Fig. S4). BFA treatment resulted in dispersion of GalT within 15 minutes (Fig. 5, supplementary material Movies 4 and 5) and of Arf1 within 3 minutes (supplementary material Fig. S4, Movies 6 and 7) as expected from prior reports (Vasudevan et al., 1998; Klausner et al., 1992). Palmitoylation-deficient GAD65(C30,45A)-GFP was dispersed from Golgi membranes upon addition of BFA at a slower rate than Arf1 (supplementary material Fig. S4, Movie 6) but similar to that of GalT (Fig. 5A, supplementary material Movie 4). Although some wt GAD65 dispersed similarly to GalT, a fraction of the protein remained visible in larger structures in the perinuclear region 15 and 30 minutes after addition of BFA (Fig. 5B, supplementary material Fig. S4, Movies 5 and 7). These structures were not observed for the palmitoylation-deficient protein. Thus, the live-cell experiments in BFA-treated cells suggest that palmitoylated GAD65 segregates into membrane domains characterized by slow dispersion following BFA treatment.

During prolonged incubation in BFA, the cation-independent mannose-6-phosphate receptor (CI-M6PR) accumulates in large irregular structures that form from the TGN (Wood et al., 1991). Consistent with a localization in the TGN, palmitoylated GAD65 was found to colocalize with CI-M6PR in such structures in fixed cells following a 1 hour BFA treatment (supplementary material Fig. S5). Taken together, the results above provide strong evidence that palmitoylation results in targeting of GAD65-GFP to TGN membrane microdomains and subsequent transit to a post-Golgi vesicular pathway.

### FRAP analyses of wt GAD65-GFP trafficking in Golgi membranes reveals two pools of protein with different kinetics

We next determined whether palmitoylation results in different kinetics of GAD65 trafficking into Golgi membranes. We analyzed the rate of replenishment of wt and palmitoylation-deficient GAD65-GFP fluorescence onto Golgi membranes after the Golgi pool was photobleached in living cells. The FRAP protocol used for these studies was similar to that developed to analyze replenishment of NRAS and HRAS in the Golgi complex

**Fig. 4.** Palmitoylation results in spatially distinct localization of GAD65-GFP in Golgi membranes of rat hippocampal neurons and increased colocalization with the *trans*-Golgi marker TGN38. High-resolution projected confocal images of rat hippocampal neurons at DIV10 transiently expressing either palmitoylation-deficient (A,B) or wild-type (C,D) GAD65-GFP. Neurons were double immunolabeled for GFP and either the *trans*-Golgi network protein TGN38 (A,C) or *cis*-Golgi matrix protein GM130 (B,D). Palmitoylation-deficient GAD65 segregates from both TGN38 (A) and GM130 (B) and appears to be oriented more proximal to the cytosol than the two markers. Wild-type GAD65-GFP, however, colocalizes with TGN38 (C) but segregates from GM130 (D) albeit to a distinct face of GM130 than palmitoylation-deficient GAD65. GAD65-GFP-containing vesicles are observed for wt GAD65 (arrowheads) but not palmitoylation-deficient GAD65. (E) Correlation coefficient (*r*) for colocalization of palmitoylation-deficient and wt GAD65-GFP with TGN38. Only wt GAD65-GFP colocalizes significantly with TGN38 (*r*=0.80±0.02). Results are presented as mean ± s.d. for 10 cells for each protein. *$P<0.001$.



(Goodwin et al., 2005). FRAP experiments were performed on live hippocampal neurons (Fig. 6), COS-7 cells (Fig. 7) and MDCK cells (supplementary material Movies 8 and 9). Cells were transfected with either wt or palmitoylation-deficient GAD65-GFP. The GFP fusion protein in the entire area of the Golgi compartment was irreversibly photobleached by a high-power focused laser beam. The recovery of fluorescence from outside the bleach region and into the photobleached area was recorded at low laser power. Analysis of the data was performed using non-linear regression, assuming one or multiple site binding.

The experiments revealed that the replenishment of palmitoylation-deficient GAD65(C30,45A)-GFP into the bleached area was monophasic in all three cell types (Figs 6, 7 and supplementary material Movie 8), occurring rapidly and completely. Thus, the half-time of fluorescence recovery (50% of plateau) was 1.7±0.2 seconds (mean ± s.e.; *n*=5; each experiment represents five cells) in neurons (Fig. 6A,C-E) and 5.3±1.6 seconds (mean ± s.e.; *n*=4; each experiment represents 5-10 cells) in COS-7 cells (Fig. 7A,C-E). The recovery of wt GAD65-GFP, by contrast, was biphasic in all three cell types (Figs 6, 7 and supplementary material Movie 9). There was a rapidly recovering pool, showing a half-time recovery of 0.6±0.3 seconds (mean ± s.e.; *n*=5; each experiment represents 5-10 cells) in neurons and constituting 62.7±3.1% of the protein, and a pool of slow recovery with a half-time of 154.3±72.1 seconds constituting 28.3±2.3% of the protein in neurons (Fig. 6B-E). In COS-7 cells, the half-time of fluorescence recovery for the rapidly recovering pool was 2.5±0.4 seconds (mean ± s.e.; *n*=4; each experiment represents 5-10 cells) constituting 53.9±4.1% of the protein, and a pool of slow recovery with a half-time of 182.4±28.7 seconds constituting 42.7±5.9% of the protein (Fig. 7B-E). Similar results were obtained in MDCK cells (supplementary material Movies 8 and 9 and results not shown). In COS-7 cells, palmitoylation-deficient protein achieved full recovery (102.2±3.1%, Fig. 7E), suggesting that there is no immobilized fraction of non-palmitoylated GAD65 on Golgi membranes of COS-7 cells. The combined recovery of wt GAD65-GFP from both the rapid and slow pools (~97%) in COS-7 cells reached near-prebleach intensities, suggesting that an immobilized fraction of wt GAD65 on Golgi membranes is either very small or non-existent. Similar results were obtained in MDCK cells (supplementary material Movies 8 and 9 and results not shown). In neurons, the recovery of the palmitoylation-deficient GAD65 and the combined recovery of the rapid and slow pools of wt GAD65 on Golgi membranes was closer to 90%. Although it cannot be excluded that the lower calculated recovery in neurons is indicative of a small immobile fraction of GAD65 in Golgi membranes of neurons, it is more likely to be due to the
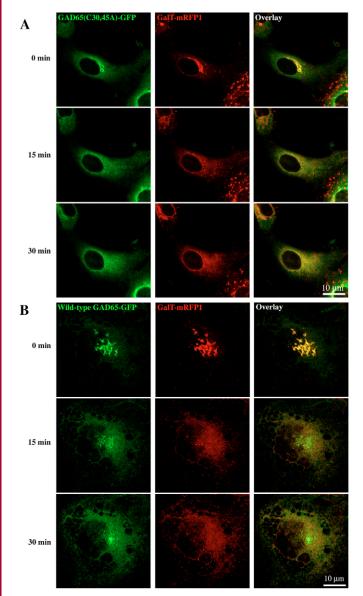
**Fig. 5.** Dispersion of the Golgi pool of palmitoylation-deficient GAD65-GFP but not wt GAD65-GFP following treatment with BFA. Selected single-layer confocal images obtained from a live-cell imaging time series recorded immediately after the addition of BFA (5 μg/ml) to COS-7 cells coexpressing GalT-mRFP1 and either the palmitoylation-deficient GAD65(C30,45A)-GFP (A) or wt GAD65-GFP (B). (A) BFA treatment has resulted in the complete dissociation of the Golgi pools of both GAD65(C30,45A)-GFP and GalT-mRFP1 at the 15 minute time-point following treatment with BFA (see also supplementary material Movie 4). Note that the cell in the lower right corner has protein aggregates because of overexpression, precluding analyses of the effect of BFA. (B) The Golgi pool of GalT-mRFP1 has redistributed to the ER at the 15 minute time-point following exposure to BFA (5 μg/ml). By contrast, only a fraction of the Golgi pool of wild-type GAD65-GFP has dispersed at 15 and 30 minutes, and a prominent fraction of the protein is still detected in punctate structures in the perinuclear region at those timepoints (see also supplementary material Movie 5). The effect of BFA is global and the cells shown in A and B are representative of cells transfected with palmitoylation-deficient GAD65-GFP and wt GAD65-GFP, respectively. Note that GAD65-containing cytosolic vesicles are not visible in the single confocal layer selected for imaging of the Golgi compartment.

inherent difficulty in measuring the loss of total cell fluorescence in the irregularly shaped neuron, resulting in an underestimation

of the correction factor (see Materials and Methods). The results suggest that two pools of wt GAD65 replenish the Golgi compartment in all three cell types. One pool rapidly exchanges on and off Golgi membranes at a rate resembling that of the palmitoylation-deficient protein. The second pool replenishes the Golgi at a half-time that is ~260 times slower in neurons and ~70 times slower in COS-cells than the fast pool.

The palmitoylation-deficient GAD65-GFP protein and the rapidly recovering portion of the wt protein both repopulated the photobleached Golgi within 1 minute and with a half-time of less than 1 second in neurons and only a few seconds in COS-7 cells. By contrast, the rates of vesicular transport from the ER to the Golgi of transmembrane proteins, such as VSVG-GFP and GalT-GFP (Hirschberg et al., 1998; Ward et al., 2001), involve tens of minutes. Therefore, we surmised that recovery of GAD65 did not occur by vesicular transport. Rather, the rates of recovery of the fast pools of GAD65-GFP and GAD65(C30,45)-GFP were similar to the rates of cytosol to Golgi membrane trafficking of the Golgi matrix protein GRASP65-GFP, of the Golgi coat protein, εCOP-GFP (Ward et al., 2001) and of the palmitoylation mutants of GFP-HRAS and GFP-NRAS (Goodwin et al., 2005). These proteins exchange continually between Golgi membranes and cytoplasmic pools in a non-vesicular fashion. The half-time of recovery of the slow pool of GAD65-GFP (2.5-3 minutes), is still orders of magnitude faster than the turnover of biosynthesis of wt GAD65 (Christgau et al., 1991), which has a half-life of 20-30 hours, suggesting that recycling, rather than de novo biosynthesis, supplies the slow pool of GAD65. The rate of recovery of the slow pool of wt GAD65 is also several fold faster than for proteins recycling back to the Golgi complex from peripheral membranes by a vesicular pathway (Nichols et al., 2001).

### The slowly recovering Golgi pool of GAD65 is dependent on palmitoylation

The half-time of recovery of the slower pool of wt GAD65 was intermediary between the half-time of recovery of singly palmitoylated NRAS and doubly palmitoylated HRAS in Golgi membranes following photobleaching as measured by Rocks et al. (Rocks et al., 2005). This rate of recovery is similar to the rate of depalmitoylation of HRAS and several other palmitoylated proteins by the cytosolic mammalian depalmitoylation enzyme acyl-protein thioesterase 1 (Duncan and Gilman, 1998; Duncan and Gilman, 2002; Yeh et al., 1999; Veit and Schmidt, 2001). NRAS and HRAS are recycled from the plasma membrane to the Golgi complex by a non-vesicular pathway, following depalmitoylation (Goodwin et al., 2005). We speculated that the slowly replenishing pool of GAD65-GFP in Golgi membranes represents palmitoylated protein that is redirected out of a post-Golgi vesicular pathway by depalmitoylation to be recycled back to the Golgi compartment as has been reported for NRAS and HRAS (Rocks et al., 2005; Goodwin et al., 2005). To test whether this pool of GAD65-GFP was indeed dependent on palmitoylation, we analyzed the effect of an inhibitor of palmitoylation, 2-bromo-palmitic acid (2-BP), on the rate of recovery of wt and palmitoylation-deficient GAD65-GFP in Golgi membranes following photobleaching in neurons and COS-7 cells. Inhibition of palmitoylation by 2-BP did not affect the kinetics of recovery of the palmitoylation-deficient GAD65(C30,45A)-GFP protein in either cell type, nor did it affect the rapidly transiting pool of wt GAD65-GFP (Fig. 8) consistent with this pool representing non-palmitoylated GAD65. However,
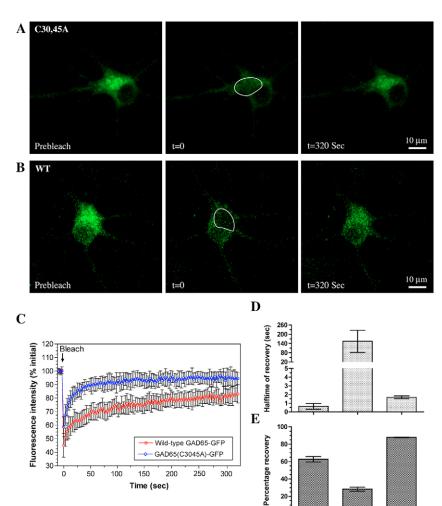
in the presence of 2-BP, the slow pool of wt GAD65-GFP disappeared, and the recovery became monophasic in both neurons and COS-7 cells, resulting in a rapid and complete replenishment of Golgi membranes with a half-time of 1.7±0.4 seconds in neurons (Fig. 8B-D) and 2.6±0.4 seconds in COS-7 cells (Fig. 8F-H). Thus, the slowly recovering pool of wt GAD65 is lost upon inhibition of re-palmitoylation, providing evidence that GAD65 in this pool is dependent on palmitoylation. The results demonstrate that the rapid pool of wt GAD65 is independent of palmitoylation and provide further evidence that this pool represents hydrophobic but non-palmitoylated GAD65 that cycles continuously on and off Golgi membranes (Form F2 in Fig. 1).
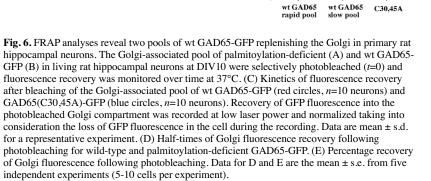
## Inhibition of palmitoylation results in disappearance of wt GAD65-GFP from cytosolic vesicles and its accumulation in the ER

We addressed the question whether 2-BP treatment affects trafficking of wt GAD65-GFP to vesicular-like puncta. High-resolution confocal analyses of wt GAD65-GFP in fixed COS-7 cells at different time points following addition of 2-BP showed a gradual disappearance of the protein from vesicular-like puncta and a gradual appearance in the ER, whereas Golgi fluorescence remained relatively unaltered. Thus, after 5 hours of inhibition by 2-BP, wt GAD65-GFP was rarely detected in vesicular-like puncta and was located almost exclusively in the ER and Golgi compartments (Fig. 9B, enlarged frames c and d, Fig. 9D,E) similar to the palmitoylation mutant (Fig. 9C, enlarged frames e and f). Thus, inhibition of palmitoylation results in accumulation of GAD65 in the ER-Golgi complex, disappearance from the vesicular pathway and disappearance of the pool that slowly replenishes the Golgi compartment.

The recycling of NRAS and HRAS to the Golgi compartment is not affected by nocodazole under conditions in which microtubules are disrupted, but the Golgi compartment has not yet fragmented, suggesting that 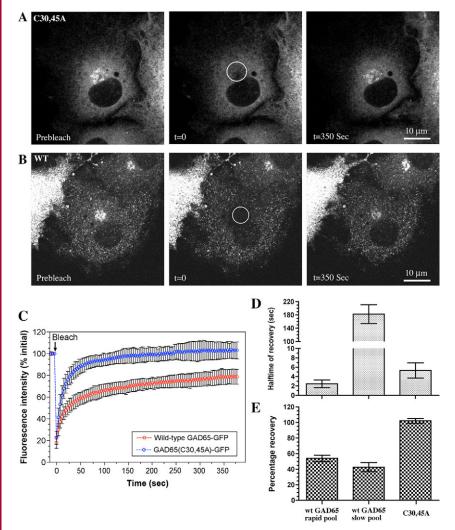trafficking of the molecules to the Golgi is independent of microtubules (Goodwin et al., 2005). We tested the effect of microtubule disruption on the recovery of GAD65-GFP fluorescence onto Golgi membranes. Immediately prior to photobleaching of the Golgi compartment, cells were cooled briefly on ice to depolymerize microtubules and then rewarmed to 37°C in the presence of nocodazole. In these conditions, the Golgi compartment was not disrupted during the FRAP analyses. The kinetics of recovery of the palmitoylation mutant and the rapidly recycling pool of wt GAD65 were not affected by microtubule disruption (supplementary material Fig. S6), providing evidence that similarly to NRAS and HRAS, trafficking of non-palmitoylated and palmitoylated GAD65 to the Golgi compartment occurs by a microtubule-independent pathway.

**Fig. 6.** FRAP analyses reveal two pools of wt GAD65-GFP replenishing the Golgi in primary rat hippocampal neurons. The Golgi-associated pool of palmitoylation-deficient (A) and wt GAD65-GFP (B) in living rat hippocampal neurons at DIV10 were selectively photobleached (*t*=0) and fluorescence recovery was monitored over time at 37°C. (C) Kinetics of fluorescence recovery after bleaching of the Golgi-associated pool of wt GAD65-GFP (red circles, *n*=10 neurons) and GAD65(C30,45A)-GFP (blue circles, *n*=10 neurons). Recovery of GFP fluorescence into the photobleached Golgi compartment was recorded at low laser power and normalized taking into consideration the loss of GFP fluorescence in the cell during the recording. Data are mean ± s.d. for a representative experiment. (D) Half-times of Golgi fluorescence recovery following photobleaching for wild-type and palmitoylation-deficient GAD65-GFP. (E) Percentage recovery of Golgi fluorescence following photobleaching. Data for D and E are the mean ± s.e. from five independent experiments (5-10 cells per experiment).

## Discussion

The data presented here suggest a trafficking pathway for GAD65 involving successive translocations from the cytosol, first to the ER-Golgi, next to the TGN and then to post-Golgi vesicles, mediated by a palmitoylation-regulated recycling node that may serve to modulate GABA synthesis by GAD65 at the neuronal synapse. We present evidence that: (1) GAD65 anchors to both ER and Golgi membranes prior to palmitoylation; (2) palmitoylation clears the protein from ER membranes and targets it to the TGN and a vesicular pathway; and (3) two distinctive pools of GAD65 differentially traffic to the Golgi compartment. The rapidly transiting pool is independent of palmitoylation and probably represents a reversible cytosol to membrane binding of a

**Fig. 7.** FRAP analyses reveal two pools of wt GAD65-GFP replenishing the Golgi in COS-7 cells. The Golgi-associated pool of palmitoylation-deficient (A) and wt GAD65-GFP (B) in living COS-7 cells were selectively photobleached (circle, *t*=0) and fluorescence recovery was monitored over time at 37°C. Note the presence of wt GAD65-GFP in cytosolic punctate structures, whereas the mutant protein is localized in the ER network of membranes. (C) Kinetics of fluorescence recovery after bleaching of the entire Golgi-associated pool of wild-type GAD65-GFP (red circles, *n*=10 cells) and GAD65(C30,45A)-GFP (blue circles, *n*=10 cells). Recovery of GFP fluorescence into the photobleached Golgi compartment was recorded at low laser power and normalized taking into consideration the loss of GFP fluorescence in the whole cell during the recording. Data are presented as mean ± s.d. from a representative experiment. (D) Half-times of Golgi fluorescence recovery following photobleaching for wild-type and palmitoylation-deficient GAD65-GFP. (E) Percentage recovery of Golgi fluorescence following photobleaching. Data for D and E are presented as mean ± s.e. from four independent experiments (5-10 cells per experiment).

containing GAD65 in all three cell types included in this study, are distinct from the axon specific Rab5a-positive EEA1-negative vesicles that harbor GAD65 in neurons (Kanaani et al., 2004) (results not shown). The cytosolic vesicles may intersect with the Rab5a pathway once they reach the axon. Depalmitoylation of GAD65 along the post-Golgi pathway (Step C) converts it back to F2, which recycles to ER-Golgi membranes by a microtubule-independent pathway, enabling a new cycle of palmitoylation and targeting to the post-Golgi vesicular transport pathway.

hydrophobic but non-palmitoylated GAD65. The more slowly transiting pool is dependent on palmitoylation and is too rapid to represent retrograde protein trafficking via a vesicular pathway. It is independent of microtubules as is the recycling of NRAS and HRAS to Golgi membranes. Based on these characteristics, as well as the similarities between the half-time of trafficking of the slow pool of GAD65 into the Golgi compartment and the half-time of recycling of palmitoylated HRAS and NRAS into Golgi, which again closely reflects the kinetics of enzymatic depalmitoylation, we propose that the slow pool represents palmitoylated GAD65 that undergoes depalmitoylation, release from the vesicular pathway and recycling back to the Golgi compartment.

The working model for GAD65 can now be expanded to include cycling between cytosol, ER-Golgi, TGN and a post-Golgi vesicular transport pathway as shown in Fig. 10. The hydrophobic non-palmitoylated GAD65, Form 2 (F2), reversibly associates with both ER and Golgi membranes, establishing an equilibrium between membrane and cytosolic pools. Following palmitoylation (Step B), catalyzed by a palmitoyl transferase (PAT) in Golgi membranes, the palmitoylated protein (F3) is targeted to the TGN, shifting the equilibrium from the ER and toward the Golgi complex. From the TGN, the protein is sorted into cytosolic vesicles that initiate a pathway to synaptic vesicles and presynaptic termini in neurons. Our preliminary results suggest that the cytosolic vesicles

**A depalmitoylation-repalmitoylation cycle as a mechanism for dynamic distribution of proteins between the Golgi compartment and peripheral membrane compartments**

A depalmitoylation-repalmitoylation cycle was first shown to regulate the localization of HRAS and NRAS between Golgi membranes and the cytosolic face of plasma membranes (Rocks et al., 2005; Goodwin et al., 2005). Two signals, farnesylation and palmitoylation, cooperate to target NRAS and HRAS to the plasma membrane (Hancock et al., 1989; Hancock et al., 1990). The farnesylated proteins have a low membrane avidity and cycle on and off ER-Golgi membranes (Choy et al., 1999; Rocks et al., 2005; Goodwin et al., 2005). Palmitoylation of one cysteine in NRAS and two cysteines in HRAS results in trapping of the proteins on the cytosolic face of Golgi membranes, targeting them to an exocytic post-Golgi vesicular pathway for delivery to the cytosolic face of the plasma membranes. Depalmitoylation results in a release from the vesicular pathway and plasma membrane, retrograde trafficking by a non-vesicular mechanism and subsequent repalmitoylation in ER-Golgi. The repalmitoylation re-anchors NRAS and HRAS on Golgi membranes and enables the protein to undergo vesicular transport back to the plasma membrane (Rocks et al., 2005; Goodwin et al., 2005). A de/repalmitoylation cycle has also been suggested to regulate the distribution of GAP43, Giα1 and eNOS between the Golgi

**Fig. 8.** The slowly recovering pool of GAD65-GFP in Golgi membranes is dependent on palmitoylation in both neurons and COS-7 cells. FRAP analysis of the Golgi-associated pool of GAD65(C30,45A)-GFP and wild-type GAD65-GFP in hippocampal neurons (A-D) and COS-7 cells (E-H). Transfected cells were treated for 5 hours at 37°C with either 25 μM 2-BP or DMSO followed by selective photobleaching of the Golgi-associated pools. (A,B,E,F) Kinetics of recovery of GFP fluorescence for palmitoylation-deficient GAD65(C30,45A)-GFP (A,E) and wt GAD65-GFP (B,F). Data for neurons are presented as mean ± s.d. ($n$=10 cells for each condition). Data for COS-7 cells are presented as mean ± s.d. ($n$=5 cells for each condition). (C,G) Half-times of recovery of Golgi fluorescence following photobleaching of wild-type and palmitoylation-deficient GAD65-GFP in the presence and absence of 2-BP. The slow phase of GAD65-GFP recovery in Golgi membranes is abolished in the presence of 2-BP. (D,H) Percentage recovery of Golgi fluorescence following photobleaching. Data for C and D are presented as mean ± s.e. ($n$=10 neurons for each condition). Data for G and H are presented as mean ± s.e. ($n$=5 COS-7 cells for each condition).

(Christgau et al., 1992). This step constitutes an alternative hydrophobic modification resulting in a reversible membrane association that both precedes and enables palmitoylation in the Golgi compartment and is analogous to the role of farnesylation in NRAS and HRAS. Step A, however, appears to invoke distinct membrane-anchoring properties from farnesylated but non-palmitoylated NRAS and HRAS. A membrane-trapping model of palmitoylation (Shahinian and Silvius, 1995; Smotrys and Linder, 2004) has been proposed to explain the two-step membrane-anchoring mechanisms of mammalian RAS proteins (Hancock et al., 1990) and heterotrimeric G-proteins (Michaelson et al., 2002). In this model, farnesylated or myristoylated (but nonpalmitoylated) proteins cycle on and off membranes until they encounter a membrane with an appropriate membrane-targeting receptor. Palmitoyl transferase (PAT) has been suggested as a candidate for such a receptor. A transient interaction with PAT leads to palmitoylation and results in trapping of the protein in membranes for as long as the protein remains palmitoylated (for a review, see Smotrys and Linder, 2004). For many proteins, however, palmitoylation in the Golgi compartment does not seem to be involved in membrane anchoring, but instead serves the function of mediating targeting to a particular post-Golgi membrane compartment. For instance, palmitoylation of the SNARE protein SNAP25 and the neuronal growth-cone associated protein GAP43 is not required for membrane binding but is essential for sorting of the two proteins at the TGN into vesicles that are delivered to their appropriate subcellular localization in the axon (for a review, see
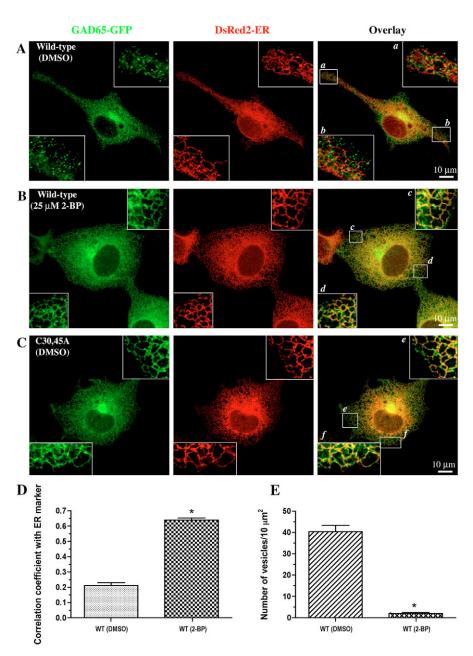
compartment and plasma membranes (Rocks et al., 2005). Our results indicate that a palmitoylation cycle analogously regulates the distribution of GAD65 between the Golgi compartment and post-Golgi membranes. Thus, a palmitoylation-depalmitoylation cycle may provide a general mechanism for dynamic cycling of proteins between the Golgi compartment and different post-Golgi peripheral membranes.

### Membrane-targeting versus membrane-anchoring roles for palmitoylation

The initial hydrophobic modification of GAD65 (Fig. 10, step A) is irreversible (Christgau et al., 1991) and involves residues 24-31 (Shi et al., 1994). It was shown not to involve polyisoprenylation, myristoylation, palmitoylation or a phosphatidylinositol glycan

**Fig. 9.** GAD65-GFP accumulates in the ER and Golgi and is absent from cytosolic vesicles in the presence of 2-BP. (A-C) High-resolution projected confocal images of COS-7 cells expressing the ER-marker DsRed2-ER together with either wild-type (A,B) or palmitoylation-deficient (C) GAD65-GFP. Transfected COS-7 cells were allowed to express the protein for 16 hours and then treated with 25 μM 2-BP (B) or DMSO (A,C) for 5 hours at 37°C before fixation and immunofluorescence analysis. Wild-type GAD65-GFP is present in cytosolic vesicles and Golgi in the absence of 2-BP and does not colocalize with DsRed2-ER (A, enlarged frames *a* and *b*). However, inhibition of palmitoylation results in the disappearance of wt GAD65-GFP from cytosolic vesicles and accumulation in ER membranes (B, enlarged frames *c* and *d*), a localization similar to that shown for the palmitoylation-deficient GAD65-GFP (C, enlarged frames *e* and *f*). (D) Correlation coefficient for colocalization of wt GAD65-GFP with the DsRed2-ER marker following incubation with a solvent (DMSO) and 2-BP, respectively. Results are presented as mean ± s.e. (*n*=10 cells per condition). *$P<0.001$. (E) Quantification of wt GAD65-GFP positive vesicles in the cytosol of COS-7 cells treated with solvent (DMSO) and 2-BP. Results are presented as mean ± s.e. (*n*=5 cells per condition). *$P<0.001$.



Bijlmakers and Marsh, 2003). The current data available for GAD65 suggest that it belongs to this latter category given the lack of evidence that palmitoylation is involved in its membrane anchoring (see below).

## Membrane-bound and soluble forms of GAD65

Because palmitoylated GAD65 is only detected in the firmly membrane-anchored pool of the protein, it was originally proposed to be critically involved in membrane anchoring, in analogy with the mammalian RAS proteins (Christgau et al., 1992). However, subcellular fractionation experiments of transfected COS-7 cells co-expressing either recombinant wt GAD65 or palmitoylation-deficient GAD65(C30,45A) proteins with HRAS, did not support a direct role of palmitoylation in membrane anchoring of GAD65 (Shi et al., 1994). In subcellular fractionation experiments, farnesylated but palmitoylation-deficient HRAS is found primarily in soluble hydrophobic fractions following a high-salt wash of membranes, whereas wt HRAS remains membrane bound (Hancock et al., 1989; Hancock et al., 1990; Shi et al., 1994). By contrast, the wt GAD65 and GAD65(C30,45A) proteins distribute similarly between soluble hydrophobic and membrane-bound fractions following high-salt wash, suggesting that they share similar membrane avidity (Shi et al., 1994). Thus, although the palmitoylated F3 form in Fig. 10 is a part of the firmly membrane-anchored pool of GAD65, the subcellular fractionation experiments suggest that hydrophobic but non-palmitoylated GAD65 also contributes to this pool. Furthermore, in contrast to the RAS proteins (Prior et al., 2001), detergent titration experiments have not revealed significant differences in solubility of membrane bound wt and palmitoylation-deficient GAD65 (our

unpublished results), suggesting that palmitoylation does not have a demonstrable effect on the membrane avidity of GAD65. One must therefore invoke an additional step occurring in the Golgi membranes, which serves to firmly anchor the hydrophobic but non-palmitoylated protein F2 to Golgi membranes prior to palmitoylation. Alternatively, differences in membrane-anchoring properties between recombinant wt and palmitoylation-deficient GAD65 may have gone undetected in biochemical analyses of subcellular fractions of COS-7 cells. We have observed that GAD65 can form aggregates when overexpressed. Although confocal analyses circumvent this problem by selecting cells with modest expression, subcellular fractionation and detergent titration experiments of transfected COS-7 cell cultures will necessarily include cells overexpressing the protein. Thus, detergent solubility experiments may not adequately distinguish between a fraction of protein that is insoluble because of high membrane affinity, and an aggregated protein that sediments with membranes.
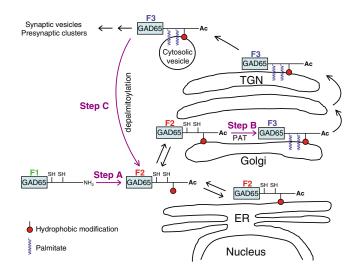
**Fig. 10.** Schematic model of GAD65 cycling between the cytosol, the ER-Golgi and a vesicular pathway. Newly synthesized hydrophilic and soluble GAD65 (F1) undergoes an irreversible hydrophobic modification in the cytosol (Step A). The resulting hydrophobic GAD65 (F2) reversibly associates with ER and Golgi membranes, establishing an equilibrium between membrane and cytosolic pools. In Golgi membranes, the protein undergoes palmitoylation (Step B) catalyzed by a palmitoyl transferase (PAT). The palmitoylated protein (F3) is targeted to the TGN, shifting the equilibrium from the ER towards the Golgi. From the TGN, the protein is targeted to cytosolic vesicles and a pathway to synaptic vesicles and presynaptic termini in neurons and synaptic-like microvesicles in pancreatic β cells. A depalmitoylation along this pathway (Step C) results in a reversal to F2, trafficking back to ER-Golgi membranes by a microtubule-independent pathway, and a new cycle of palmitoylation and targeting to the vesicular pathway.

## Palmitoylation as a targeting signal in GAD65

Although the weight of current evidence suggests that palmitoylation does not play a critical role in membrane anchoring of GAD65, previous studies (Kanaani et al., 2002; Kanaani et al., 2004) and the results presented herein unequivocally demonstrate a critical role of palmitoylation in subcellular targeting of this enzyme. It has been proposed that non-palmitoylated NRAS and HRAS attach indiscriminately to intracellular membranes and that their trapping in Golgi membranes is determined by the Golgi location of its PAT (Rocks et al., 2005). Other studies, however, have been consistent with a specific association of farnesylated but non-palmitoylated NRAS with ER-Golgi membranes (Choy et al., 1999) and this appears to be the case for non-palmitoylated GAD65. Thus, palmitoylation-deficient GAD65(C30,45A)-GFP is detected solely in ER-Golgi membranes. GAD65 has been shown to be a substrate for HIP-14 (Huang et al., 2004). In addition to the Golgi compartment, this PAT is localized widely on recycling and late endosomal compartments where GAD65 is absent. HIP-14 is, therefore, an unlikely factor in determining the membrane specificity of GAD65 targeting. Rather, the Golgi localization signal in GAD65 in residues 1-23 (Kanaani et al., 2002) may function independently of a PAT. It is conceivable, however, that palmitoylation by HIP-14 in Golgi membranes mediates the shift of GAD65 to the TGN.

## Is the palmitoylation-depalmitoylation cycle important for the function of GAD65?

There is now a compelling body of evidence indicating that the GAD65 isoform is critical for incremental synthesis of GABA to produce rapid responses to environmental stimuli (Tian et al., 1999; Patel et al., 2006). Cycling of the enzyme between inactive apoenzyme and active holoenzyme, regulated by levels of PLP, is likely to provide one level of regulating GABA syntheses in presynaptic terminals. The palmitoylation-depalmitoylation cycle identified in this study may be an intricate part of a mechanism to direct cytosolic and Golgi pools of the enzyme to presynaptic termini to sustain GABA production for rapid secretion. Thus, it may prove an instrumental part of the specific role of GAD65 in inhibitory neurotransmission. Our preliminary FRAP experiments in hippocampal neurons, suggest that the replenishing of GAD65 in presynaptic termini in a resting neuron, is monophasic and has a half-time (~50 seconds) of the same order of magnitude as the half-time of the slow phase of GAD65-replenishing Golgi membranes. Thus trafficking of GAD65 into presynaptic clusters is several orders of magnitude faster than trafficking of transmembrane proteins from ER-Golgi to peripheral membranes by vesicular transport. The emerging picture is that a palmitoylation-depalmitoylation cycle provides a rapid mechanism for regulating the distribution of proteins between the Golgi and peripheral membranes. It will be important to show the functional significance of the acylation cycle in GABAergic neurons and its role in regulation of inhibitory neurotransmission.

## Materials and Methods

### Antibodies

The following antibodies were used in immunofluorescence experiments: mouse monoclonal antibodies to the Golgi matrix protein of 130 kDa (GM130) and to the *trans*-Golgi network protein of 85-95 kDa with core polypeptide of 38 kDa (TGN38) were from BD Biosciences (Palo Alto, CA). Rabbit polyclonal antibody against the C-terminal residues 472-618 of human CDP cut alternatively spliced protein (Gillingham et al., 2002) was kindly provided by Sean Munro (MRC LMB, Cambridge, UK). Rabbit polyclonal antibody to the hemagglutinin (HA) epitope tag was from Covance/BABCO (Berkeley, CA) and chicken polyclonal antibody raised to purified 6-his tagged GFP was from Chemicon (Temecula, CA). Rabbit polyclonal antibody to the cation-independent mannose-6-phosphate receptor (CI-M6PR) was kindly provided by Frances Brodsky (University of California, San Francisco, CA). Cy3-conjugated AffiniPure donkey anti-mouse IgG was purchased from Jackson ImmunoResearch Laboratories (West Grove, PA). Alexa Fluor 488 goat antibodies against rabbit or chicken IgG were from Molecular Probes (Eugene, OR).

### DNA constructs

Chimeras containing EGFP at the C-terminal end of either wild-type GAD65 or a palmitoylation-deficient mutant GAD65(C30,45A) were described earlier (Kanaani et al., 2002). The fusion protein containing EGFP at the N-terminus of dominant negative mutant (S34N) of human Rab5a in pEGFP-C3 was provided by Ruth Collins (Cornell University, NY). The C-terminal fusion protein of the HA tag and VGAT (VGAT-HA) in the mammalian expression vector pcDNA3 was from Robert Edwards, UCSF. The fusion protein containing the pH-sensitive mutant of GFP (ecliptic pHluorin) joined to VAMP2/synaptobrevin at its lumenally exposed C-terminus (synapto-pHluorin) in the pCI mammalian expression vector, was kindly provided by James Rothman, Memorial Sloan Kettering Cancer Center, NY (Miesenböck et al., 1998). The mammalian expression vector containing mRFP1 was prepared by PCR amplification using the N-terminal primer 5′-GATCGGATCCA-CCGGTCGCCACCATGGCCTCCTCCGAG-3′ containing a *Bam*HI site (underlined) and the C-terminal primer 5′-GATCCGCGGCCGCTTTAGGCGCCGGTGGAG-3′ containing a *Not*I site (underlined) using the pRSETB-mRFP1 (gift from Roger Tsien, UCSD, San Diego, CA) as template. The amplification product was gel purified, digested with the restriction endonucleases, *Bam*HI and *Not*I, and ligated into a similarly digested pEGFP-N1 (Clontech Laboratories) to produce the mRFP1-N1 expression plasmid. The GalT-mRFP1 constructed by removing an *Xho*I-*Bam*HI digested fragment from pEGFP-N1-GalT containing the Golgi targeting domain previously described (Cole et al., 1996) and subcloning it into a similarly digested mRFP1-N1. The Arf1-mRFP1 constructed by removing an *Xho*I-*Bam*HI digested fragment from pEGFP-N1-Arf1 (Vasudevan et al., 1998) and subcloning it into a similarly digested mRFP1-N1. The mammalian expression vector, pDsRed2-ER, which encodes a fusion consisting of *Discosoma sp.* red fluorescent protein (DsRed2), the endoplasmic reticulum (ER) targeting sequence of calreticulin fused to the 5′ end of DsRed2, and the ER retention sequence KDEL fused to the 3′ end of DsRed2, was purchased from Clontech.

## Cell culture and transfection

Preparation of primary cultures of rat hippocampal neurons from embryonic day 18/19 rats was performed according to published protocols (Brewer et al., 1993). Briefly, hippocampal neurons, dissociated with papain and brief mechanical trituration, were maintained in neurobasal medium (Invitrogen Corporation, Grand Island, NY) supplemented with B27, penicillin (100 U/ml), streptomycin (100 µg/ml), Glutamax-1 (0.5 mM), and β-mercaptoethanol (25 µM; Sigma-Aldrich). Hippocampal cultures were transfected at day-in-vitro (DIV) 6-7 using the Effectene lipid-mediated gene transfer kit (QIAGEN Sciences, Maryland). After 2-3 hours of incubation at 37°C, the transfection solution was replaced with a 50:50 solution of fresh/conditioned medium (replacement medium). COS-7 cells were cultured in Dulbecco's modified Eagle's medium (DMEM) supplemented with 10% fetal bovine serum, glutamine (2 mM) and penicillin-streptomycin. MDCK cells were cultured in minimal essential medium (MEM) containing Earle's salts and supplemented with 10% fetal bovine serum, glutamine (25 µM) and penicillin/streptomycin. COS-7 cells were transfected using LipofectAMINE Plus Reagent and MDCK cells were transfected using LipofectAMINE 2000 reagent according to the manufacturer protocol (GIBCO). After 5 hours of incubation at 37°C, the transfection solution was replaced with fresh culture medium. For experiments with BFA (Sigma-Aldrich), a 5 mg/ml stock solution was prepared in ethanol. BFA was diluted in culture medium and added to COS-7 cells 16 hours after transfection to a final concentration of 2 µg/ml and incubated for 1 hour at 37°C before fixation of cells. Golgi and microtubule disruption of COS-7 cells was carried out 16 hours after transfection by addition of nocodazole (Sigma-Aldrich) at a final concentration of 20 µg/ml followed by incubation for 5 hours at 37°C. Cells were then fixed and analyzed by immunofluorescence. Inhibition of protein palmitoylation in COS-7 cells was carried out by incubation with 25 µM 2-bromopalmitate (2-BP, Sigma-Aldrich) either immediately after transfection followed by incubation for 16 hours at 37°C or 16 hours after transfection with incubation times of 30, 60, 150 and 300 minutes at 37°C. Control experiments were performed using the vehicle DMSO at 1:400 dilution. Cells were fixed and analyzed by immunofluorescence.

## Immunofluorescence analyses

For indirect immunofluorescence, cells were plated on poly-D-lysine-treated glass coverslips (12 mm in diameter; Electron Microscopy Sciences, Ft. Washington, PA) in 24-well plates (Falcon). Neuronal cultures were fixed 48-72 hours after transfection with 2% paraformaldehyde (PFA) in phosphate buffered saline (PBS), pH 7.4. COS-7 and MDCK cells were fixed 17-24 hours after transfection with 2% PFA. A chicken polyclonal anti-GFP antibody (Chemicon) was used as a primary antibody to enhance the signal of GFP-chimeras in neuronal transfections. Fixed cells were first washed with PBS and then blocked for 20 minutes with blocking solution (2% normal goat serum, 0.3% TX-100 in PBS). Cells were incubated with primary antibodies in blocking solution for 1 hour at room temperature, washed with PBS, and then incubated with appropriate fluorochrome-conjugated secondary antibodies in blocking solution for 1 hour at room temperature. After washing with PBS, the coverslips were mounted on slides (Frost Plus, Fisher) with Fluoromount-G (Southern Biotechnology Associates, Birmingham, AL). Fluorescent images were obtained using a Leica TCS NT laser-scanning confocal microscope with a Krypton-Argon laser (Leica Microsystems, Wetzlar, Germany). All confocal images were derived from 8-10 consecutive horizontal optical sections estimated at 0.2-0.5 µm in thickness. For multichannel imaging, fluorescent dyes were imaged sequentially in frame-interlace mode, to eliminate cross talk between the channels.

The measurement of the correlation between the average pixel intensities of GAD65-GFP and the ER marker DsRed2-ER, the *trans*-Golgi marker TGN38, and the *cis*-Golgi marker GM130 was performed using the correlation plot application in MetaMorph software (Universal Imaging Company, Downingtown, PA). In the first set of experiments, the analysis was performed on projected confocal images of COS-7 cells co-transfected with either wt or palmitoylation-deficient GAD65-GFP and DsRed2-ER. In the second set of experiments, the analysis was performed on projected confocal images of rat hippocampal neurons transfected with either wt or palmitoylation-deficient GAD65-GFP and immunostained for endogenous TGN38 or GM130. A region of approximately 10 µm$^2$ was drawn on the image with red fluorescence (DsRed2-ER, TGN38, and GM130) and then this image was thresholded prior to the measurement, so that only pixels that have intensities that are outside of the threshold range of both GAD65-GFP and either DsRed2-ER, TGN38 or GM130 images were excluded from the measurement. This measurement was repeated in four different areas per cell and the average calculated. A total of 10 cells from two separate experiments were analyzed per condition. For every image pixel being analyzed, Metamorph examines the intensity of the corresponding pixels in the two images, and uses the two intensity values as the *x* and *y* coordinates in the scatterplot. The correlation coefficient (*r*) of the data is defined as $r=\Sigma\ xy/NSx\ Sy$, where *r*=correlation coefficient, *xy*=product of deviation scores, *N*=sample size, S*x*=standard deviation of *x* (intensities in first image), and S*y*=standard deviation of *y* (intensities in second image).

Quantification of the number of GAD65-GFP-containing vesicles in the cytosol of transfected COS-7 cells was performed manually on projected confocal images of COS-7 cells using Improvision Openlab software. The number of vesicles was counted in an area of approximately 10 µm$^2$ and was repeated five times per cell for a total of five cells per condition. Results of quantification were analyzed by a *t*-test using a two-tailed distribution and two-sample equal variance.

## Live-cell imaging and photobleaching

For live-cell experiments, rat hippocampal neurons, COS-7 and MDCK cells were cultured in Lab-Tek chambers with 1.0 borosilicate cover glasses (Nalge Nunc International, Naperville, IL) or on 1.5 round cover glasses (A. Daigger & Company, Wheeling, IL). Hippocampal neurons were transfected at DIV 7 using Effectene reagent and live-cell imaging was carried out at DIV 10 in neurobasal medium without Phenol Red. COS-7 cells were transfected using FuGENE 6 transfection reagent (Roche, Indianpolis, IN) and MDCK cells were transfected using LipofectAMINE 2000 reagent. Live-cell experiments of COS-7 and MDCK cells were performed 24-48 hours after transfection in DMEM as above without Phenol Red and containing 25 mM HEPES pH 7.5 (Biosource International, Rockville, MD). For live imaging of COS-7 cells during the BFA treatment, BFA was diluted to 50 µg/ml in imaging medium and added to cells at final concentration of 5 µg/ml just prior to beginning of the imaging experiment. For disruption of microtubules but not Golgi in COS-7 cells, the cell culture medium was changed to ice-cold imaging medium containing 5 µg/ml nocodazole and cells were cooled on ice for 10 minutes. The cell culture medium was then changed to 37°C imaging medium containing 5 µg/ml nocodazole and FRAP experiments were performed 5 minutes later in the continued presence of nocodazole at 37°C to prevent polymerization of new microtubules. Control experiments were performed using vehicle alone (DMSO). For inhibition of palmitoylation, 2-BP was added to hippocampal neurons at a final concentration of 25 µM, 56 hours after transfection and to COS-7 cells 16 hours after transfection. Cells were incubated with 2-BP or the vehicle, DMSO, for 5 hours at 37°C prior to FRAP analysis.

FRAP experiments of rat hippocampal neurons were carried out using Leica TCS SP2 laser scanning confocal microscope with Acousto-optical beam splitters (AOBS) and HCX PL APO 63×/1.20 water objective (Leica Microsystems, Wetzlar, Germany). The FRAP experiments were performed on a heated stage adjusted to 37°C and contained within a moisturized and CO$_2$-controlled box. Image format of 512×512 pixels and line averaging with two iterations was used, which led to a 3.26 second image scan time. Photobleaching was performed with a 3.26 second pulse of high level of 488 nm laser light and region of interest (ROI) zoom-in bleach function was activated to increase the bleaching power. Fluorescence emission was collected at 3.26 second intervals with a 498-600 nm emission range filter through a completely open pinhole of the 63× objective. Live-cell imaging and FRAP experiments of COS-7 and MDCK cells were performed in multi-tracking mode on a Zeiss LSM510 laser scanning confocal microscope (Carl Zeiss, Thornwood, NY) with a 63× Plan Apochromat 1.4 NA objective or 25× 0.8 NA Plan NeoFluar objective, a 413/488 dichroic mirror, and the 488 nm line of an argon ion laser (Lasos, Germany) with intensity levels (~1-3 µW) measured at the rear aperture of the objective. Pixel time was ~1.6 µsecond and images were line averaged (four iterations) which led to ~4 second image scan time. Photobleaching was performed with a ~3 second pulse of high level (~1-1.5 mW) of 488 nm laser light measured at the rear aperture of the objective. Fluorescence emission was collected at ~4 second intervals with a 505 nm long-pass filter through a pinhole selected for an approximate 1 µm optical slice when using the 63× objective and an approximate 21.4 µm slice when using the 25× objective.

The images of neurons were analyzed using the Leica confocal software (LCS) (Leica Microsystems, Wetzlar, Germany) and of COS-7 and MDCK cells using the Zeiss LSM510 physiology software (Carl Zeiss, Thornwood, NY), by drawing a region of interest around the Golgi region, a region of interest around the entire cell, and a region of interest outside the cell (representing background). The mean pixel values within the regions of interest were determined for each time point. The background values were subtracted from the Golgi and whole cell values. The values were normalized to the levels corresponding to the image prior to the photobleaching pulse. To accurately estimate the fraction of molecules associating/disassociating with the Golgi apparatus, the recovery of the Golgi region was normalized for the decrease in total cell fluorescence as determined from the measurement of the whole cell region of interest. Half-times of recovery and the percentage of recovered fluorescence were calculated using GraphPad Prism 4 software (GraphPad Software, San Diego, CA). Analysis of the data was performed using non-linear regression, assuming one- or two-site binding.

Live-cell imaging of COS-7 cells during the BFA experiments was performed in multi-tracking mode on a Zeiss LSM510 laser-scanning confocal microscope with a 63× Plan Apochromat 1.4 NA objective and a 488/543 dichroic mirror. The GFP was excited with the 488 nm line and the mRFP1 was excited with a 543 nm HeNe (Lasos, Germany). Pixel time was ~1.6 µseconds and images were line averaged (eight iterations) which led to a ~16 second image scan time. Images were collected at 30 second intervals with the autofocus routine (Carl Zeiss, Thornwood, NY) every 10 minutes. GFP emission was collected with a 505-550 nm bandpass filter. RFP1 emission was collected with a 560 nm longpass filter. The pinholes for each channel were set for an approximate 1 µm optical slice.

# References

**Asada, H., Kawamura, Y., Maruyama, K., Kume, H., Ding, R., Ji, F. Y., Kanbara, N., Kuzume, H., Sambo, M., Yagi, T. et al.** (1996). Mice lacking the 65 kDa isoform of glutamic acid decarboxylase (GAD65) maintain normal levels of GAD67 and GABA in their brains but susceptible to seizures. *Biochem. Biophys. Res. Commun.* **229**, 891-895.

**Asada, H., Kawamura, Y., Maruyama, K., Kume, H., Ding, R. G., Kanbara, N., Kuzume, H., Sanbo, M., Yagi, T. and Obata, K.** (1997). Cleft palate and decreased brain gamma-aminobutyric acid in mice lacking the 67-kDa isoform of glutamic acid decarboxylase. *Proc. Natl. Acad. Sci. USA* **94**, 6496-6499.

**Baekkeskov, S., Aanstoot, H. J., Christgau, S., Reetz, A., Solimena, M., Cascalho, M., Folli, F. and Richter-Olesen, H.** (1990). Identification of the 64K autoantigen in insulin-dependent diabetes as the GABA-synthesizing enzyme glutamic acid decarboxylase. *Nature* **347**, 151-156.

**Battaglioli, G. H., Liu, H. and Martin, D. L.** (2003). Kinetic differences between the isoforms of glutamate decarboxylase: implications for the regulation of GABA synthesis. *J. Neurochem.* **86**, 879-887.

**Battaglioli, G., Liu, H., Hauer, C. R. and Martin, D. L.** (2005). Glutamate decarboxylase: Loss of N-terminal segment does not affect homodimerization and determination of the oxidation state of cysteine residues. *Neurochem. Res.* **30**, 989-1001.

**Bijlmakers, M. and Marsh, M.** (2003). The on-off story of palmitoylation. *Trends Cell. Biol.* **13**, 32-42.

**Brewer, G. J., Torricelli, J. R., Evege, E. K. and Price, P. J.** (1993). Optimized survival of hippocampal neurons in B27-supplemented neurobasal, a new serum-free medium combination. *J. Neurosci. Res.* **35**, 567-576.

**Chege, N. W. and Pfeffer, S. R.** (1990). Compartmentation of the Golgi complex: brefeldin-A distinguishes trans-Golgi cisternae from the trans-Golgi network. *J. Cell Biol.* **111**, 893-899.

**Choy, E., Chiu, V. K., Silletti, J., Feoktistov, M., Morimoto, T., Michaelson, D., Ivanov, I. E. and Philips, M. R.** (1999). Endomembrane trafficking of Ras: The CAAX motif targets proteins to the ER and Golgi. *Cell* **98**, 69-80.

**Christgau, S., Schierbeck, H., Aanstoot, H. J., Aagaard, L., Begley, K., Kofod, H., Hejnaes, K. and Baekkeskov, S.** (1991). Pancreatic β-cells express two autoantigenic forms of glutamic acid decarboxylase, a 65kDa hydrophilic form and a 64kDa amphiphilic form which can be both membrane-bound and soluble. *J. Biol. Chem.* **266**, 21257-21264.

**Christgau, S., Aanstoot, H. J., Schierbeck, H., Begley, K., Tullin, S., Hejnaes, H. and Baekkeskov, S.** (1992). Membrane anchoring of the autoantigen GAD65 to microvesicles in pancreatic β-cells by palmitoylation in the N-terminal domain. *J. Cell Biol.* **118**, 309-320.

**Cole, N. B., Sciaky, N., Marotta, A., Song, T. and Lippincott-Schwartz, J.** (1996). Golgi dispersal during microtubule disruption regeneration of Golgi stacks at peripheral endoplasmic reticulum exit sites. *Mol. Biol. Cell* **7**, 631-650.

**Condie, B. G., Bain, G., Gottlieb, D. I. and Capecchi, M. R.** (1997). Cleft palate in mice with a targeted mutation in the gamma-aminobutyric acid-producing enzyme glutamic acid decarboxylase 67. *Proc. Natl. Acad. Sci. USA* **94**, 11451-11455.

**Duncan, J. A. and Gilman, A. G.** (1998). A cytoplasmic acyl-protein thioesterase that removes palmitate from G protein alpha subunits and p21RAS. *J. Biol. Chem.* **273**, 15830-15837.

**Duncan, J. A. and Gilman, A. G.** (2002). Characterization of Saccharomyces cerevisiae acyl-protein thioesterase 1, the enzyme responsible for G protein alpha subunit deacylation in vivo. *J. Biol. Chem.* **277**, 31740-31752.

**Gillingham, A. K., Pfeifer, A. C. and Munro, S.** (2002). CASP, the alternatively spliced product of the gene encoding the CCAAT-displacement protein transcription factor, is a Golgi membrane protein related to Giantin. *Mol. Biol. Cell* **13**, 3761-3774.

**Goodwin, J. S., Drake, K. R., Rogers, C., Wright, L., Lippincott-Schwartz, J., Philips, M. R. and Kenworthy, A. K.** (2005). Depalmitoylated Ras traffics to and from the Golgi complex via a nonvesicular pathway. *J. Cell Biol.* **170**, 261-272.

**Hancock, J. F., Magee, A. I., Childs, J. E. and Marshall, C. J.** (1989). All ras proteins are polyisoprenylated but only some are palmitoylated. *Cell* **57**, 1167-1177.

**Hancock, J. F., Paterson, H. and Marshall, C. J.** (1990). A polybasic domain or palmitylation is required in addition to the CAAX motif to localize p21ras to the plasma membrane. *Cell* **63**, 133-139.

**Hensch, T. K., Fagiolini, M., Mataga, N., Stryker, M. P., Baekkeskov, S. and Kash, S.** (1998). Local GABA circuit control of experience-dependent plasticity in developing visual cortex. *Science* **282**, 1504-1508.

**Hirschberg, K., Miller, C. M., Ellenberg, J., Presley, J. F., Siggia, E. D., Phair, R. D. and Lippincott-Schwartz, J.** (1998). Kinetic analysis of secretary protein traffic and characterization of Golgi to plasma membrane transport intermediates in living cells. *J. Cell Biol.* **143**, 1485-1503.

**Huang, K., Yanai, A., Kang, R., Arstikaitis, P., Singaraja, R. R., Metzler, M., Mullard, A., Haigh, B., Guathier-Campbell, C., Gutekunst, C. et al.** (2004). Huntingtin-Interacting Protein HIP14 is a palmitoyl transferase involved in palmitoylation and trafficking of multiple neuronal proteins. *Neuron* **44**, 977-986.

**Kanaani, J., El-Husseini, A. E., Aguilera-Moreno, A., Diacovo, M. J., Bredt, D. S. and Baekkeskov, S.** (2002). A combination of three distinct trafficking signals mediates axonal targeting and presynaptic clustering of GAD65. *J. Cell Biol.* **158**, 1229-1238.

**Kanaani, J., Diacovo, M. J., El-Husseini, A. E., Bredt, D. and Baekkeskov, S.** (2004). Palmitoylation controls trafficking of GAD65 from Golgi membranes to axon-specific endosomes and a Rab5a-dependent pathway to presynaptic clusters. *J. Cell Sci.* **117**, 2001-2013.

**Kash, S. F., Johnson, R. S., Tecott, L. H., Noebels, J. L., Mayfield, R. D., Hanahan, D. and Baekkeskov, S.** (1997). Epilepsy in mice deficient in the 65-kDa isoform of glutamic acid decarboxylase. *Proc. Natl. Acad. Sci. USA* **94**, 14060-14065.

**Kash, S. F., Tecott, L. H., Hodge, C. and Baekkeskov, S.** (1999). Increased anxiety and altered responses to anxiolytics in mice deficient in the 65 kDa isoform of glutamic acid decarboxylase. *Proc. Natl. Acad. Sci. USA* **96**, 1698-1703.

**Klausner, R. D., Donaldson, J. G. and Lippincott-Schwartz, J.** (1992). Brefeldin A: insights into the control of membrane traffic and organelle structure. *J. Cell Biol.* **116**, 1071-1080.

**Lippincott-Schwartz, J., Yuan, L., Tipper, C., Amherdt, M., Orci, L. and Klausner, R. D.** (1991). Brefeldin A's effects on endosomes, lysosomes, and the TGN suggest a general mechanism for regulating organelle structure and membrane traffic. *Cell* **67**, 601-616.

**Michaelson, D., Aheran, I., Bergo, M., Young, S. and Phillips, M.** (2002). Membrane trafficking of heterotrimeric G proteins via the endoplasmic reticulum and Golgi. *Mol. Biol. Cell* **13**, 3294-3302.

**Miesenböck, G., De Angelis, D. A. and Rothman, J. E.** (1998). Visualizing secretion and synaptic transmission with pH-sensititve green fluorescent proteins. *Nature* **394**, 192-195.

**Namchuk, M., Lindsay, L. A., Turck, C. W., Kanaani, J. and Baekkeskov, S.** (1997). Phosphorylation of Serine Residues 3, 6, 10, and 13 distinguishes membrane anchored from soluble glutamic acid decarboxylase 65 and is restricted to glutamic acid decarboxylase 65α. *J. Biol. Chem.* **272**, 1548-1557.

**Nichols, B. J., Kenworthy, A. K., Polishchuk, R. S., Lodge, R., Roberts, T. H., Hirschberg, K., Phair, R. D. and Lippincott-Schwartz, J.** (2001). Rapid cycling of lipid raft markers between the cell surface and Golgi complex. *J. Cell Biol.* **153**, 529-541.

**Patel, A. B., deGraaf, R. A., Martin, D. L., Battaglioli, G. and Behar, K. L.** (2006). Evidence that GAD65 mediates increased GABA synthesis during intense neuronal activity in vivo. *J. Neurochem.* **97**, 385-396.

**Prior, I. A., Harding, A., Yan, J., Sluimer, J., Parton, R. G. and Hancock, J. F.** (2001). GTP-dependent segregation of H-ras from lipid rafts is required for biological activity. *Nat. Cell Biol.* **3**, 368-375.

**Reetz, A., Solimena, M., Matteoli, M., Folli, F., Takei, K. and DeCamilli, P.** (1991). GABA and pancreatic β-cells: colocalization of glutamic acid decarboxylase (GAD) and GABA with synaptic like microvesicles suggests their role in GABA storage and secretion. *EMBO J.* **10**, 1275-1284.

**Rocks, O., Peyker, A., Kahms, M., Verveer, P. J., Koerner, C., Lumbierres, M., Kuhlmann, J., Waldmann, H., Wittinghofer, A. and Bastiaens, P. I. H.** (2005). An acylation cycle regulates localization and activity of palmitoylated ras isoforms. *Science* **307**, 1746-1752.

**Shahinian, S. and Silvius, J. R.** (1995). Doubly-lipid-modified protein sequence motifs exhibit long-lived anchorage to lipid bilayer membranes. *Biochemistry* **34**, 3813-3822.

**Shi, Y., Veit, B. and Baekkeskov, S.** (1994). Amino acid residues 24-31 but not palmitoylation of cysteines 30 and 45 are required for membrane anchoring of glutamic acid decarboxylase, GAD65. *J. Cell Biol.* **124**, 927-934.

**Shimura, T., Watanabe, U., Yanagawa, Y. and Yamamoto, Y.** (2004). Altered taste function in mice deficient in the 65-kDa isoform of glutamate. *Neurosci. Lett.* **356**, 171-174.

**Smotrys, J. E. and Linder, M. E.** (2004). Palmitoylation of intracellular signaling proteins: regulation and function. *Annu. Rev. Biochem.* **73**, 559-587.

**Solimena, M., Folli, F., Aparisi, G., Pozza, G. and De Camilli, P.** (1990). Autoantibodies to GABA-ergic neurons and pancreatic beta cells in stiff-man syndrome. *N. Engl. J. Med.* **322**, 1555-1560.

**Solimena, M., Dirkx, R., Radzynski, M., Mundigl, O. and De Camilli, P.** (1994). A signal located within amino acids 1-27 of GAD65 is required for its targeting to the Golgi complex region. *J. Cell Biol.* **126**, 331-341.

**Stork, O., Ji, F. Y., Kaneko, K., Stork, S., Yoshinobu, Y., Moriya, T., Shibata, S. and Obata, K.** (2000). Postnatal development of a GABA deficit and disturbance of neural functions in mice lacking GAD65. *Brain Res.* **865**, 45-58.

**Stork, O., Yamanaka, H., Stork, S., Kume, N. and Obata, K.** (2003). Altered conditioned fear behavior in glutamate decarboxylase 65 null mutant mice. *Genes Brain Behav.* **2**, 65-70.

**Tian, N., Petersen, C., Kash, S., Baekkeskov, S., Copenhagen, D. and Nicoll, R.** (1999). The role of the synthetic enzyme GAD65 in the control of neuronal γ-aminobutyric acid release. *Proc. Natl. Acad. Sci. USA* **96**, 12911-12916.

**Vasudevan, C., Han, W., Tan, Y., Nie, Y., Li, D., Shome, K., Watkins, S. C., Levitan, E. S. and Romero, G.** (1998). The distribution and translocation of the G protein ADP-Ribosylation factor 1 in live cells is determined by its GTPase activity. *J. Cell Sci.* **111**, 1277-1285.

**Veit, M. and Schmidt, M. F. G.** (2001). Enzymatic depalmitoylation of viral glycoproteins with acyl-protein thioesterase 1 *in vitro*. *Virology* **288**, 89-95.

**Ward, T. H., Polishchuk, R. S., Caplan, S., Hirschberg, K. and Lippincott-Schwartz, J.** (2001). Maintenance of Golgi structure and function depends on the integrity of ER export. *J. Cell Biol.* **155**, 557-570.

**Wood, S. A., Park, J. E. and Brown, W. J.** (1991). Brefeldin A causes a microtubule-mediated fusion of the *trans*-Golgi network and early endosomes. *Cell* **67**, 591-600.

**Yeh, D. C., Duncan, J. A., Yamashita, S. and Michel, T.** (1999). Depalmitoylation of endothelial nitric-oxide synthase by acyl-protein thioesterase 1 is potentiated by $Ca^{2+}$-calmodulin. *J. Biol. Chem.* **274**, 33148-33154.